C. R. Physique 3 (2002) 1121–1130

Physique subatomique/*Subatomic physics*

AVANCÉES EN PHYSIQUE DES PARTICULES : LA CONTRIBUTION DU LEP

ADVANCES IN PARTICLE PHYSICS: THE LEP CONTRIBUTION

Polarisation and precise calibration of the LEP beam energy

Jean-Pierre Koutchouk, Massimo Placidi

CERN, CH-1211 Geneva 23, Switzerland

Received 15 May 2002; accepted 1 July 2002

Note presented by Guy Laval.

Abstract We report in this article on two issues of precision accelerator physics, performed at the LEP collider, that challenged international collaborations. The first result is an increase of the polarisation degree from an almost vanishing natural level to 50%, opening the way to energy calibration by resonant depolarisation. The second result is a systematic and precise determination of the collider centre-of-mass energy correcting for subtle effects such as the azimuthal variation of the beam energy, the magnets temperature, the effects of parasitic earth currents and terrestrial tides. It resulted in an extremely accurate test of the Standard Model and set significant constraints on the top quark and Higgs masses. ***To cite this article: J.-P. Koutchouk, M. Placidi, C. R. Physique 3 (2002) 1121–1130.***

polarisation / spin / resonances / energy / calibration

Polarisation et calibration précise de l'énergie du LEP

Résumé Dans cet article, nous résumons deux sujets de physique d'accélérateur de précision, obtenus au collisionneur LEP, qui ont motivé des collaborations internationales. Le premier résultat est un accroissement du degré de polarisation depuis une valeur naturelle presque nulle jusqu'à 50% ouvrant la voie à la calibration d'énergie par dépolarisation résonante. Le second résultat est une calibration précise et systématique de l'énergie dans le centre de masse du collisionneur, tenant compte d'effets subtils tels que la variation azimutale de l'énergie du faisceau, les effets de température, les courants de terre parasites, les marées terrestres. Ces mesures ont permis un test extrêmement précis du Modèle Standard et des contraintes beaucoup plus précises sur les masses du quark top et du Higgs. ***Pour citer cet article : J.-P. Koutchouk, M. Placidi, C. R. Physique 3 (2002) 1121–1130.***

polarisation / spin / résonances / énergie / calibration

E-mail addresses: Jean-Pierre.Koutchouk@cern.ch (J.-P. Koutchouk); Massimo.Placidi@cern.ch (M. Placidi).

S1631-0705(02)01401-9/FLA

1. Introduction

We report in this article on two issues of precision accelerator physics, performed at the LEP collider, that challenged international collaborations: firstly an increase of the polarisation degree; and secondly a precise determination of the collider centre-of-mass energy. The authors names appear in [1–4].

The production in large numbers of the Z^0 and, to a lesser extent, of the W particles has made of LEP a unique tool for a precision test of the Standard Model. The principle is to predict some observable, such as the Z^0 width, using as input parameters the masses of the top quark, of the Higgs particle, and compare with the measurements. The accuracy of the experiment must be high enough to match the range of these electroweak corrections and allow sensitivity to new physics. The uncertainty on the energy scale is the main limitation. The requirement for the accuracy of the beam energy was estimated to be first ± 4.5 MeV [5] and later reduced to ± 1.5 MeV [6]. This is beyond what can be achieved with magnetic measurements (± 9 MeV). The most accurate method to calibrate the beam energy is by resonant depolarisation. The challenge at the LEP energies was to minimise the consequences of the strong quantum excitation enhancing the spin diffusion. The beam dynamics model indicated indeed an almost vanishing natural beam polarisation level. In this article we summarise the quest for polarisation, the principle of the resonant depolarisation and the centre-of-mass energy calibration proper. The latter is deduced from the measurement of the beam energy after very fine corrections of some subtle effects.

2. Polarisation in LEP

Polarisation and depolarising phenomena in electron and proton machines are accounted for, e.g., in [7,8]. The spontaneous Sokolov–Ternov [9] radiative polarisation of electron beams is perhaps the only example of a macroscopic beam behaviour governed by quantum-mechanical laws. Under the influence of the central acceleration of the collider magnetic field the electrons emit quantum 'synchrotron radiation' photons. A very small probability exists for an electron to experience a spin flip after quantum emission. When this is the case however, the preference for a final spin state anti-parallel to the magnetic field is very large. An electron beam becomes slowly polarised with a time constant τ_{p}.

The time evolution of the polarisation P in the vertical magnetic field of a storage ring is described by:

$$P(t) = P_{\infty}\left(1 - \mathrm{e}^{-t/\tau_{\mathrm{p}}}\right), \tag{1}$$

$$\tau_{\mathrm{p}}^{-1} = (w_{\uparrow\downarrow} + w_{\downarrow\uparrow}) = \frac{5\sqrt{3}}{8}\frac{\hbar r_{\mathrm{e}}}{m_{\mathrm{e}}}\frac{\gamma_{\mathrm{e}}^5}{\rho_{\mathrm{eff}}^3} = 0.353 \times 10^{-18}\left(\frac{\gamma_{\mathrm{e}}^5}{\rho_{\mathrm{eff}}^3}\right)\ \mathrm{s}^{-1}, \tag{2}$$

$$P_{\infty} = \frac{(w_{\uparrow\downarrow} - w_{\downarrow\uparrow})}{(w_{\uparrow\downarrow} + w_{\downarrow\uparrow})} = \frac{8}{5\sqrt{3}} = 92.4\%, \tag{3}$$

where $w_{\uparrow\downarrow}$ and $w_{\downarrow\uparrow}$ are the spin flip probabilities, m_{e} and r_{e} the electron mass and classical radius, γ_{e} the $\mathrm{e}^{\pm}$ beam Lorentz factor and ρ_{eff} the effective bending radius.

The ideal polarisation time τ_{p} ranges, for LEP, from ~ 320 min at the Z^0 peak to $\sim$10 min at 90 GeV.

2.1. Spin precession, spin-orbit coupling and depolarisation

A realistic collider does not exhibit an azimuthally homogeneous vertical magnetic field (e.g., experimental solenoids). The calculation of the actual asymptotic polarisation level is then performed by averaging the spin vectors over the beam population. For each particle the spin vector **S**, quantum average of the spin operator, precesses according to the BMT [10] equation:

$$\frac{\mathrm{d}\mathbf{S}}{\mathrm{d}t} = \Omega_{\mathrm{BMT}} \times \mathbf{S}, \tag{4}$$

$$\Omega_{\mathrm{BMT}} = -\frac{e}{m_{\mathrm{e}}\gamma_{\mathrm{e}}}\left[(1 + a_{\mathrm{e}}\gamma_{\mathrm{e}})\mathbf{B}_{\perp} + (1 + a_{\mathrm{e}})\mathbf{B}_{\parallel} - \left(a_{\mathrm{e}} + \frac{1}{1+\gamma_{\mathrm{e}}}\right)\beta_{\mathrm{e}}\gamma_{\mathrm{e}} \times \frac{\mathbf{E}}{c}\right], \tag{5}$$

where, besides the usual physical constants, $a_e = (\gamma_e - 2)/2 = 1.159\,652\,188 \times 10^{-3}$ is the $e^{\pm}$ gyromagnetic anomaly, $\mathbf{B}_\perp$ is the transverse component of the magnetic field, $\mathbf{B}_\parallel$ the axial field, e.g., from solenoids and $\mathbf{E}$ the electrical field, e.g., from the electrostatic separators in LEP.

New phenomena appear characterised by significant accelerator parameters:

- The number ν of spin precessions per revolution (spin tune) is related to the beam energy E_b averaged along the machine circumference:

$$\nu = a_e \gamma_e = \frac{E_b\ (\mathrm{GeV})}{0.4406486(1)}. \tag{6}$$

- The separation between adjacent integer spin tunes (440.1 MeV for $e^{\pm}$) is energy-independent.
- The spin dynamics can be expressed as a precession about an axis $\mathbf{n}(s)$, the equilibrium polarisation direction, variable along the machine azimuth s. Whenever $\mathbf{n}(s)$ is bent away from the main magnetic field direction, the component of the polarisation in the orthogonal plane fades away due to the spin phase mixing from the finite horizontal beam size.
- Spin-orbit coupling resonances occur whenever the spin tune is commensurate with any combination of the beam eigentunes Q:

$$\nu = k + k_x Q_x + k_y Q_y + k_s Q_s, \quad k, k_x, k_y, k_s \in \mathcal{Z}. \tag{7}$$

First-order spin resonances are well known in proton accelerators. In electron colliders, they are strongly enhanced by quantum excitation: after damping, the orbit is restored but the spin is not. The resulting depolarisation increases with the square of the ratio of the photon to the beam energy.

Numerical models for LEP anticipated no polarisation on first-order resonances and hardly any in between due to higher-order effects. Simplified analytic models predicted a polarisation level below 10%.

The depolarisation by spin diffusion is described by a depolarisation time τ_d and an effective build-up time τ_{eff} and the time evolution (1) can be written:

$$P(t) = \frac{P_\infty}{\tau_p/\tau_{eff}}\left(1 - e^{-t/\tau_{eff}}\right), \quad \frac{1}{\tau_{eff}} = \frac{1}{\tau_p} + \frac{1}{\tau_d}. \tag{8}$$

2.2. Maximisation of the polarisation at LEP

The search for polarisation in LEP was initially difficult: its natural level was comparable to the polarimeter resolution, the machine tuning for physics was unfavourable and the beam diagnostics had not yet achieved the required performance. A reliable 9% polarisation level was finally detected and a systematic improvement programme could be pursued along the following lines:

- a new optics design optimised both for physics and polarisation involving modifications in the arc cell phase advances and in the betatron tunes (integer and fractional);
- spin-matching of the experimental solenoids to restore the vertical position of the closed spin solution in the arcs by rotators made of orbit bumps (Fig. 1);
- very accurate corrections of the vertical orbit and dispersion required machine re-alignments, improvement in the beam position measurement and correction procedures and beam-based measurements of the quadrupoles–BPM's relative alignment;
- implementation of the harmonic spin matching, via the measurement of the orbit harmonics in the spin precession frame and their correction with patterns of orbit bumps. The method proved very efficient in weakening the near-by linear spin resonances and their non-linear satellites (Fig. 1).

It became gradually possible to calibrate the beam energies at the end of the physics coasts after minor changes to the machine tuning, though with only one beam. The polarisation level during the LEP normal operation at 45 GeV was routinely about 20%. The maximum achieved was $57 \pm 3\%$ at a beam energy of

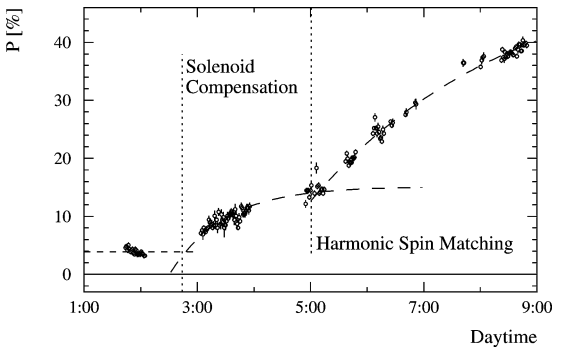

Figure 1. LEP polarisation build-up at the Z^0.

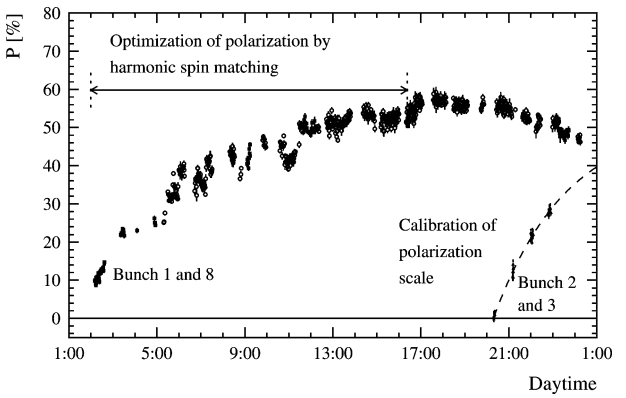

Figure 2. Maximum LEP polarisation near the Z^0.

44.7 GeV (Fig. 2). A detectable degree of polarisation was achieved up to 60 GeV above which the quantum excitation completely smeared the Sokolov–Ternov radiative process.

3. The LEP polarimeter

The fast LEP polarimeter [11], based on spin-dependent Compton scattering of *circularly* polarised photons from *transversely* polarised electrons and positrons, is schematically shown in Fig. 3.

The Klein–Nishina total cross section expressed in differential form in terms of electron and photon polarisation states in the $e^{\pm}$ *rest frame* [12,13] can be written:

$$\frac{d\sigma_c(\vec{P}_e, \vec{\xi})}{d\Omega} = \left(\frac{r_e}{\sqrt{2}}\frac{k'}{k'_0}\right)^2 \left[\Phi_0 + \Phi_1(\vec{\xi}) + \Phi_2(\vec{\xi}, \vec{P}_e)\right], \tag{9}$$

where $\vec{P}_e$ and $\vec{\xi}$ are the $e^{\pm}$ and photon polarisation vectors and k', k'_0 the scattered and incident photon momenta. When illuminating vertically polarised beams ($P_{x,z} = 0$, $P_y \equiv P_\perp$) with circularly polarised light ($\xi_{1,2} = 0$, $\xi_3 = \pm 1$) the term Φ_1 vanishes and the vertical distribution of the backscattered photons exhibits an *up-down* Compton asymmetry from the azimuthal angle ϕ' in the spin-dependent term Φ_2:

$$A_\perp = \frac{\Phi_2(\vec{\xi}, P_y)}{\Phi_0} = \xi_3 P_\perp \cdot \boldsymbol{\kappa}(\theta', \lambda_{ph}, \gamma_e) \cdot \mathbf{sin}\,\boldsymbol{\phi'} \propto \Delta\tilde{\boldsymbol{y}}. \tag{10}$$

The observable is a *shift* $\Delta\tilde{y}$ in the mean of the vertical distributions of the scattered photons. Recorded under reversal of the photon helicity, it provides a measurement of the $e^{\pm}$ polarisation level via the energy-dependent analysing power $\boldsymbol{\kappa}$ optimised by a proper choice of the photon wavelength λ_{ph}.

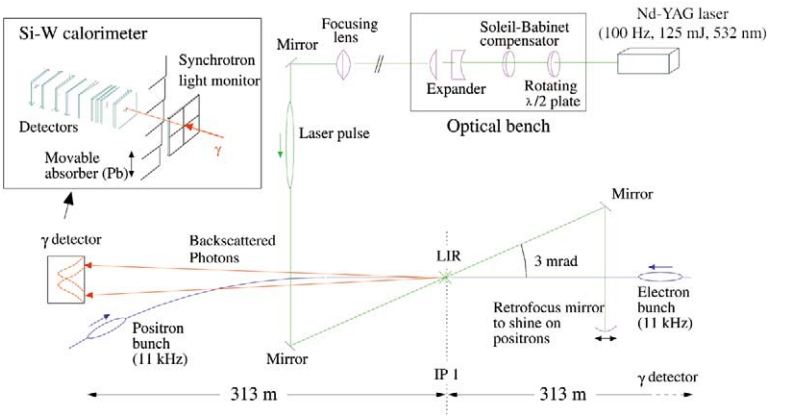

Figure 3. Schematic of the LEP Compton polarimeter.

3.1. Gamma detector and laser light control

The on-line monitoring of the time evolution of the polarisation level during the different operations and improvements was provided by two 2×16 channel, 1 mm pitch silicon strip γ-detectors located about 300 m downstream the Laser Interaction Region (LIR) (Fig. 3). Special care was devoted to the control of the polarisation state of the laser photons to avoid systematic errors. A rotating $\lambda/2$- and a $\lambda/4$-plate installed in an optical bench at the laser output produce any elliptical light state, from linear to circular. The polarimeter was initially set up using linear light as in this case the cross section (9) does not depend on beam polarisation. The correlation between the observed mean-shift reversal and real beam polarisation was checked by introducing an additional π phase-shift to intentionally reverse the photon handedness. The ellipticity of the photons was then optimised to compensate for depolarising effects from optical elements in the light path.

3.2. Calibration and performance

The analysing power κ was calibrated, at a given beam energy, by accurate determination of the effective rise time τ_{eff} and the asymptotic mean-shift from a fit to the measured time evolution (8) normalised to the actual polarisation state of the laser photons (Fig. 2). Its value at the Z^0 energy was

$$\kappa_{\text{LEP}} = \frac{\Delta\widetilde{y}}{\xi_3 P_\perp} = (4.4 \pm 0.3)\ \mu\text{m}\%^{-1} \tag{11}$$

and its accuracy was estimated to $\sim$1% in 1 minute data taking for 100% circularly polarised light.

A measurement of the width of a depolarising resonance, shown in Fig. 4, accounts for the accuracy and the resolution of the LEP polarimeter.

4. Energy calibration by resonant depolarisation

The method, developed for the VEPP2M storage ring [14] and implemented at LEP [1], derives the beam energy from the spin tune (6). The observable is the beam precession frequency

$$f_{\text{s}} = \nu f_{\text{rev}} = \big(N + [\nu]\big) f_{\text{rev}}, \tag{12}$$

where $[\nu]$ denotes the fractional part of the spin tune, whose integer part N is determined from the setting of the main bending field, and f_{rev} is the revolution frequency. When the frequency of a sweeping small amplitude radial magnetic field is in resonance with f_{s} the spin is bent away from the unperturbed vertical

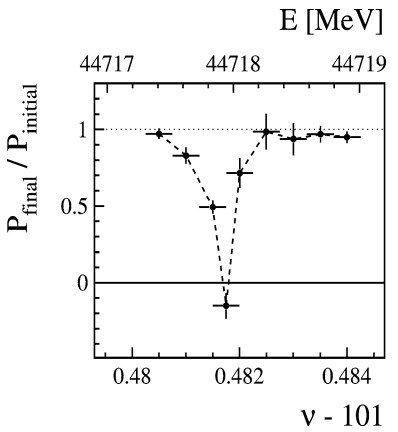

Figure 4. Width of a depolarising resonance.

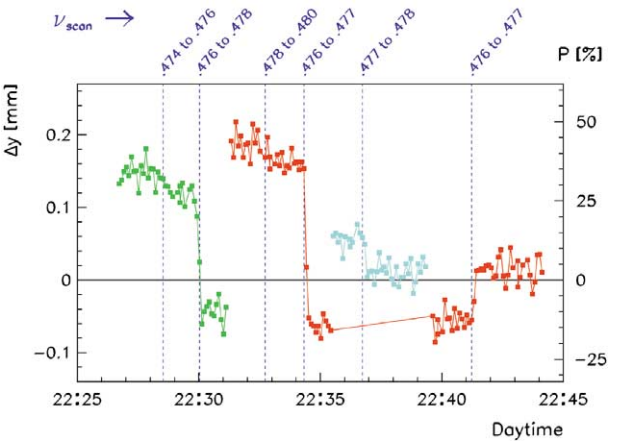

Figure 5. Energy calibration showing multiple spin flips.

direction. The beam energy, averaged over the circumference and the particles in the bunch, is then:

$$E_{\mathrm{b}} = \frac{m_{\mathrm{e}}\, c^2}{a_{\mathrm{e}}} \left(\frac{f_{\mathrm{s}}}{f_{\mathrm{rev}}} + N \right). \tag{13}$$

The 4 Gm field strength of the depolariser, provided by the LEP horizontal feedback kicker, was adjusted so as not to perturb the beam dynamics. Full depolarisation or (partial) spin flip was observed (Fig. 5) depending on the speed at which the depolarising resonance was crossed.

5. Calibration of the LEP beam energy at the Z^0

In order to measure the mass and width of the Z^0 resonance, LEP was operated at three centre-of-mass energies: 91.2 and 91.2 ± 1.8 GeV, chosen to minimise beam depolarisation. The energy calibration was mostly performed at the end of a subset of physics runs (6.4% on peak, 53.5% off peak). The electron beam energy was measured with occasional checks on the energy of the positron beam.

The analysis of the uncertainty on the Z^0 mass and width is detailed in [2] and summarised in Table 1.

5.1. Precision of the calibration of the average beam energy

The resolution, in principle limited by the uncertainty on the electron mass, was estimated to be 10^{-5} (± 0.5 MeV at the Z^0) given the adopted sweeping strategy and the time response of the polarimeter.

Systematic errors are dealt with experimentally and/or by calculation. The sampling of the spin tune at only one machine azimuth leaves an *aliasing ambiguity* ([ν] above or below a half-integer), solved by measuring the precession frequency (12) at a slightly different beam energy. Spurious resonances appearing when the exciter frequency equals the Q_{s} side-band (7) were identified by measuring f_{s} after a small change in the synchrotron tune.

As shown in (13), the method assumes a simple relationship between the beam energy and the spin tune. In practice, the spin does not always precess about the vertical axis. Spin tune shifts from the experimental solenoids, the radial fields from imperfections, the non-linear fields, the interference between the artificial and natural spin resonances were thoroughly investigated. Altogether, the systematic errors were evaluated to be 0.2 MeV *rms*. Experimental tests only provided an upper bound of 1.1 MeV [1].

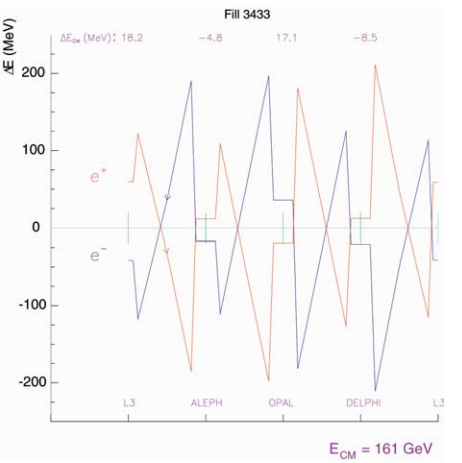

Figure 6. Energy sawtooth at $E_{\mathrm{CM}} = 161$ GeV.

5.2. From the average beam energies to E_{CM} at the experiments

The energy radiated by synchrotron radiation in the dipoles, about 125 MeV per revolution at the Z^0 energy, is replaced by local longitudinal acceleration in the RF cavities. As a result the energies of the electrons and positrons are different at a given azimuth (Fig. 6) but their sum E_{CM} should be constant. This is however not the case in LEP due to longitudinal misalignments of the RF cavities. The variation of E_{CM} depends on the losses (wigglers), RF voltage distribution, phase errors and beam loading. A detailed model of the energy gains and losses, cross-checked by measuring the synchrotron tune and azimuthal position of the collision points in the detectors, allowed the reduction of this uncertainty from up to 20 MeV down to 0.7 MeV.

Imperfections in the LEP lattice cause the electrons and positrons to travel on slightly different trajectories. The $e^{\pm}$ energy difference, estimated to less than 0.3 MeV, was confirmed when resonant depolarisation was implemented on the positron beam in 1994 and 1995.

Another source of uncertainty arose when operating LEP with bunch trains. The vertical separation required to avoid parasitic bunch collisions causes an energy dispersion at the interaction points, of opposite sign for electrons and positrons, and an E_{CM} shift occurs. The effect was minimised by accurate separation scans but could not be totally suppressed as it depends on the bunch positions in the trains. A modelling of the effect, however, allowed the reduction of the residual uncertainty.

Finally, unequal currents in the excitation bars of the quadrupole families caused a residual magnetic field of 6.6 μT on the reference beam orbit. The effect was either electrically compensated by an additional bus-bar or simply corrected from the logged unbalance of the quadrupole excitation.

5.3. From E_{CM} to the luminosity-weighted E_{CM}

If the collider energy varies along a coast, the relevant parameter is its luminosity-weighted time average. It was therefore crucial: (i) to continuously measure the variations of the beam energy during the fills; and (ii) to reproduce as accurately as possible the same machine conditions. For that purpose, the magnets were carefully cycled before each fill and eventually a fast modulation of the exciting current was applied.

Several machine parameters were recorded about 4 times per hour including the magnetic field measured in a reference magnet and in up to 16 LEP dipoles, the cooling water and dipole core temperatures and the closed orbits. In addition, an absolute calibration of the dipole field was regularly carried out by measuring the magnetic flux across a loop wired in each dipole during the magnet cycling procedure.

Table 1. Summary of sources and systematic uncertainties (MeV) on M_Z, Γ_Z and M_W after correction, from [2] and [3].

Source	ΔM_Z	$\Delta\Gamma_Z$	ΔM_W
Dipole rise model (parasitic currents, temperature)	1.5	0.5	1
Uncalibrated fills	0.5	0.8	–
Resonant depolarisation	–	0.5	1
E_{CM} versus average beam energy	0.4	0.2	2
Horizontal orbit correctors	0.2	0.1	3
e^+ energy uncertainty	0.2	0.1	2
Dispersion	0.2	0.1	2
Beam energy spread	–	0.2	
Earth tides	–	0.15	1
Quadrupole bus–bars	0.1	0.1	
Fast cycles	0.1	0.1	
Extrapolation NMR/depolarisation	–	–	11
Extrapolation NMR/flux-loop	–	–	20
Initial dipole energy	–	–	2
Optics changes	–	–	4

5.3.1. *Guide field rise during a fill*

Energy data revealed a puzzling rise of the main magnetic field corresponding to a beam energy variation of the order of 4 ± 2.6 MeV over a fill. A thorough study of the temperature behaviour of the machine dipoles was carried out, including the implementation of a test facility. The temperature variations of the magnetic cores, generated by the excitation bus-bars and synchrotron radiation and balanced by the cooling water circuit, causes small geometrical deformations of the dipoles and modifications to the iron permeability through changes in the internal stresses. The field rise was minimised by changing the cooling strategy, i.e., keeping constant the dipole temperature rather than that of the chilled water. Altogether, these effects were accurately modelled to predict their effect every 15 minutes along all runs, but only about 50% of the observed field rise could be accounted for.

The residual part of the field rise was eventually traced back to parasitic currents flowing along the LEP vacuum chamber from IP1 to IP6. A dedicated test confirmed that their time structure could alter the iron magnetisation of the dipoles causing a small but continuous energy increase. The currents were found to depend on the time of the day and their temporal evolution was finally correlated to that of leakage currents from trains travelling a few kilometres away. An algorithm predicting the energy rise from the measured parasitic currents was conceived, resulting in a 10-parameter LEP energy model used to evaluate the E_{CM} in all LEP fills. The residual uncertainty is given in Table 1.

5.3.2. *Variations of the LEP circumference*

During the energy calibration campaign the beam became occasionally depolarised without any appreciable change in the machine parameters. This effect was traced back to tiny variations in the LEP circumference due to periodic deformations of the earth crust under the gravitational influence of moon and sun (earth tides). A change in the accelerator structure induces a radial displacement of the machine components with respect to the beam orbit defined by the RF frequency. Due to the associated

energy deviation the spin tune drifts to the nearest higher-order depolarising resonance. Once the effect experimentally quantified [15] the machine energy setting could be fine-adjusted to prevent depolarisation.

After correcting for tidal forces, changes in the LEP radius by up to several 100 µm were still recorded over periods of weeks using the beam orbit measurement system. The accuracy of the latter being in the 10 µm range, regular orbit measurements were performed for energy correction. The observations were found qualitatively well correlated with the changes in the pressure of the water-table under the Jura mountains and with the water level of the Geneva lake.

5.4. The effect of the beam energy spread

The accuracy on the width Γ_Z of the Z^0 resonance is affected by the uncertainty on the centre-of mass energy spread. The resulting 1.0 MeV error on Γ_Z represented the largest systematic uncertainty in the first years of operation. The beam energy spread was thus both measured and evaluated through the logging of the wiggler excitation and the calculation of the damping distributions. The measurement is indirect, through the monitoring of the luminosity-weighted interaction length at the experiments. The knowledge of the incoherent synchrotron tune is needed to correlate bunch length and energy spread. This was initially derived from the measured coherent synchrotron tune and the evaluated machine impedance. Later, the measurement of the distance of spin resonances driven by the synchrotron motion provided more accurate results and the residual uncertainty could be reduced from 1.0 MeV to 0.2 MeV.

6. Calibration of the LEP beam energy above the W threshold

The statistical uncertainty on the W mass is set to about 25 MeV from the luminosity integrated in the four LEP experiments. The systematic error is determined by the knowledge of the beam energy which must therefore be measured to 10–15 MeV. Spin diffusion, strongly energy dependent, prevented any polarisation above 60 GeV and the resonant depolarisation method could not be used. The average beam energy was therefore determined from an estimate of the field integral derived from continuous magnetic information by 16 NMR probes installed in a small sample of the LEP dipoles. The calculation of the centre-of-mass energy in each experiment was carried out as discussed for the Z^0 measurements (Section 5). The following strategy established the relation between the NMR measurements and the beam energy:

- resonant depolarisation in the 41 to 60 GeV energy range was used to calibrate the NMR probes and to check their linearity. Over 70 points were taken along the years with excellent reproducibility. The results showed however a non-linear component of 2 MeV over 40 GeV which, although negligible, raised the issue on the model to be used to extrapolate to 90 GeV;
- a second, independent comparison was performed using the flux loop. This provides a measurement of 95.6% of the main field integral along the ring and was used to check the linearity of the NMR reading over the whole energy range;
- finally, the beam energy and spread were either predicted or evaluated from the measurement of the synchrotron tune and of the integrated RF voltage.

In contrast to the calibration at the Z^0 energy, the direct measurement of the magnetic field includes the temperature coefficient and the effect of parasitic ground currents. An energy model remains necessary to account for all the phenomena which cause the beam to travel off the central reference orbit, such as the earth tides and other geological deformations or the deliberate changes in RF frequency used to decrease the beam horizontal emittance in LEP2. The error on the W mass is dominated by the uncertainty in the extrapolation of the resonant depolarisation calibrations at lower energies.

The elaboration of the energy data at the W threshold is still on the way [16]. The analysis of the data collected until 1998 is available in [3] and summarised in Table 1.

7. Conclusion

The improved understanding and control of the spin dynamics [1,4] allowed a degree of polarisation measurable up to a beam energy of 60 GeV. This could be used for a very precise energy calibration campaign at the Z^0 peak and, with some loss in the accuracy due to the extrapolation, for a precise measurement at the W threshold.

An exceptional effort was carried out [2,3] in investigating all conceivable sources of uncertainties and data discrepancies, leading to the identification of exotic effects such as the influence of the moon phases, of the near-by train traffic and the water level of lake Geneva. This is likely to remain an example of precision physics.

When the results from all the experiments are combined, the present knowledge of Z^0 and W masses and widths is summarised as:

$$M_{\mathrm{Z}} = (91187.5 \pm 1.3_{\mathrm{exp}} \pm 1.7_{\mathrm{LEP}})\ \mathrm{MeV}, \tag{14}$$

$$\Gamma_{\mathrm{Z}} = (2495.2 \pm 2.0_{\mathrm{exp}} \pm 1.1_{\mathrm{LEP}})\ \mathrm{MeV}, \tag{15}$$

$$M_{\mathrm{W}} = (80450 \pm 36_{\mathrm{exp}} \pm 17_{\mathrm{LEP}})\ \mathrm{MeV}. \tag{16}$$

It is interesting to note that, although beam polarisation was initially only an option in LEP, it eventually contributed to one of the outstanding results. The detailed study of the systematics turned out also to require the understanding of an unexpected variety of phenomena.

References

[1] L. Arnaudon, et al., Z. Phys. C 66 (1995) 45.
[2] R. Assmann, et al., Eur. Phys. J. C 6 (1999) 187.
[3] A. Blondel, et al., Eur. Phys. J. C 11 (1999) 573.
[4] M. Böge, et al., in: Proc. EPAC '98, p. 409.
[5] G. Altarelli, et al., CERN 86-02, 1986.
[6] A. Blondel, CERN/SL92-29(DI), 1992.
[7] B. Montague, Phys. Rep. 113 (1) (1984).
[8] J. Buon, J.P. Koutchouk, CAS 1993, CERN 95-06, Vol. II, 1995.
[9] A.A. Sokolov, I.M. Ternov, Soviet Phys. Dokl. 8 (1964) 1203.
[10] V. Bargmann, L. Michel, V.L. Telegdi, Phys. Rev. Lett. 10 (1959) 435.
[11] V.N. Baier, V.A. Khoze, Soviet J. Nucl. Phys. 9 (1969) 238.
[12] U. Fano, J. Opt. Soc. Am. 39 (1949) 859.
[13] F.W. Lipps, H.A. Toelhoek, Physica XX (1954) 85 and 395.
[14] Ya. Derbenev, et al., Part. Acc. 10 (1980) 177.
[15] L. Arnaudon, et al., NIM A (1995) 249–252, 11 August 1994.
[16] G. Wilkinson (for the LEP Energy Working Group), private communication.